Chemical Enhancements in Shock-Accelerated Particles: Ab initio Simulations

Damiano Caprioli, Dennis T. Yi, and Anatoly Spitkovsky

Phys. Rev. Lett. **119**, 171101 — Published 23 October 2017

DOI: 10.1103/PhysRevLett.119.171101

Chemical Enhancements in Shock-accelerated Particles: Ab-initio Simulations

Damiano Caprioli,[1,2] Dennis T. Yi,[2] and Anatoly Spitkovsky[2]

[1]*Department of Astronomy and Astrophysics, University of Chicago, Chicago, IL 60637, USA*
[2]*Department of Astrophysical Sciences, Princeton University, Princeton, NJ 08544, USA*

(Dated: September 11, 2017)

We study the thermalization, injection, and acceleration of ions with different mass/charge ratios, A/Z, in non-relativistic collisionless shocks via hybrid (kinetic ions–fluid electrons) simulations. In general, ions thermalize to a post-shock temperature proportional to A. When diffusive shock acceleration is efficient, ions develop a non-thermal tail whose extent scales with Z and whose normalization is enhanced as $(A/Z)^2$, so that incompletely-ionized heavy ions are preferentially accelerated. We discuss how these findings can explain observed heavy-ion enhancements in Galactic cosmic rays.

PACS numbers: 95.85.Ry, 96.50.Pw, 96.50.sb, 96.50.Vg, 96.50.Fm, 98.38.Mz

Introduction.— Non-relativistic shocks are often associated with energetic particles. Prominent examples are the blast waves of supernova remnants (SNRs), likely the sources of Galactic cosmic rays (GCRs) [e.g., 1–3], and heliospheric shocks, the sources of solar energetic particles (SEPs). Chemical abundances in GCRs and SEPs provide crucial information about the processes responsible for their acceleration.

The chemical composition of GCRs is roughly solar at trans-relativistic energies [4], except for secondaries produced by spallation of primary GCRs. A more careful analysis reveals that the GCR composition is controlled by the first ionization potential, volatility, and mass/charge ratios: refractory elements show larger enhancements than volatile ones, and heavier volatile elements are more abundant than lighter ones [4–6]. At TeV energies, where spallation is negligible, the fluxes of H, He, C-N-O, and Fe are comparable [e.g., 7], despite their typical solar number abundances relative to H being $\chi_{He} = 0.0963$, $\chi_{CNO} = 9.54 \times 10^{-4}$, $\chi_{Fe} = 8.31 \times 10^{-5}$ [8]; therefore, heavy ions must be preferentially accelerated compared to protons. Chemical enhancements in SEPs, instead, greatly vary from event to event [e.g., 9, 10] and crucially depend on the presence of pre-existing energetic seed particles in the solar wind [e.g., 11, 12].

In this Letter we use —for the first time— kinetic plasma simulations to investigate the chemical enhancements of particles energized via diffusive shock acceleration (DSA) [13, 14]. Previous studies were mostly based on either analytical or Monte Carlo approaches [see, e.g, 7, 15, 16], the only few examples of hybrid simulations with heavy ions being some pioneering 1D simulations of weak shocks including $\alpha-$particles [17, 18] and the recent study of the thermalization of weakly-charged ions [19]. Since our ab-initio simulations do not include energetic seeds, we expect them to be directly relevant to GCRs accelerated in SNRs and to represent a benchmark for the analysis of the more complex SEP phenomenology.

Hybrid simulations.— We performed 2D kinetic simulations with *dHybrid*, a massively parallel hybrid code, in which ions are treated kinetically and electrons as a neutralizing fluid [20]. Hybrid simulations of non-relativistic shocks have been already used for assessing the efficiency of proton DSA [21], the generation of magnetic turbulence due to plasma instabilities [22], the diffusion of energetic particles [23], and the injection of protons into the DSA process [24].

Here we include additional ion species characterized by number abundances χ_i, atomic mass A_i, and charge Z_i (in proton units), initially in thermal equilibrium with protons. We fix $\chi_{i\neq H} = 10^{-5}$ to make ions other than protons dynamically unimportant. The electron pressure is a polytrope with an effective adiabatic index chosen to satisfy the shock jump conditions with thermal equilibration between downstream protons and electrons [24].

Lengths are measured in units of c/ω_p, where c is the speed of light and $\omega_p \equiv \sqrt{4\pi ne^2/m}$, with m, e and n the proton mass, charge and number density; time is measured in units of $\omega_c^{-1} \equiv mc/eB_0$, B_0 being the strength of the initial magnetic field; velocities are normalized to the Alfvén speed $v_A \equiv B/\sqrt{4\pi mn}$, and energies to $E_{sh} \equiv mv_{sh}^2/2$, with v_{sh} the velocity of the upstream fluid in the downstream frame. We account for the three spatial components of the particle momentum and of the electromagnetic fields. Shocks are produced as in [21] and are characterized by their Mach number M, which represents both the sonic and the Alfvénic one. The shock inclination is defined by the angle ϑ between the direction of $\mathbf{B}_0$ and the shock normal.

The time-step is chosen as $\Delta t = 0.01/M\omega_c^{-1}$ and the computational box measures $2.5 \times 10^4 c/\omega_p$ by $2Mc/\omega_p$, with two cells per ion skin depth. The numerical heating that can arise in long-term simulations with species of disparate physical density is controlled by protons, while heavier ions behave as tracers and do not heat up if the overall noise level is low; therefore, we use 100 protons per cell to minimize heating, and only 4 particles per cell for other ions. We have checked the convergence of our main results against 3D simulations, time and space resolution, number of particles per cell, and box size [see

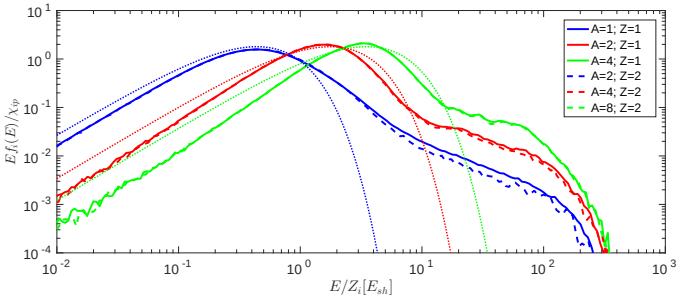

FIG. 1: Normalized post-shock spectra for ion species with mass A and charge Z as in the legend, for a quasi-parallel ($\vartheta = 20°$) shock with $M = 10$. The thermal peaks correspond to the Maxwellian distributions (color-matching dotted lines) expected if the temperature scaled with A; the non-thermal tails have a maximum extent $\propto E/Z$ and a normalization enhanced as a function of A/Z.

also 21, 22, for more tests].

Our benchmark case comprises ion species with $A = \{1, 2, 4, 8\}$ and $Z = \{1, 2\}$ and a quasi-parallel ($\vartheta = 20°$) shock with $M = 10$, which exhibits efficient proton DSA and magnetic field amplification [21, 22]: $\sim 10\%$ of the shock kinetic energy is converted into accelerated protons, and the field is amplified by a factor of $\gtrsim 2$ in the upstream. The downstream ion spectra are shown in Fig. 1, as a function of E/Z and normalized to their abundances χ_i. The color code indicates A/Z, while solid and dashed lines correspond to $Z = 1$ and 2.

Every species shows a thermal peak plus the universal DSA momentum spectra $f(p) \propto p^{-4}$, corresponding to $f(E) \propto E^{-3/2}$ at non-relativistic energies [21]. Non-thermal spectra roll over at an energy $E_{max,i}$, which increases linearly with time [23]. For strong shocks, Rankine–Hugoniot conditions return a downstream thermal energy $\mathcal{E} \simeq 0.6 E_{sh}$ [21]. Since half of the post-shock proton energy goes into electron heating by construction, we expect $\mathcal{E}_H \simeq \mathcal{E}/2$. Then, since heavier ions have more kinetic energy to convert into thermal energy, their temperature is expected to scale with their masses, i.e., $\mathcal{E}_{i\neq H} = A_i \mathcal{E}$. Dotted lines in Fig. 1 correspond to Maxwellian distributions with such expected temperatures: they provide a good fit for the positions of thermal peaks, but only a rough one for the shape of the thermal distributions of heavy ions, whose relaxation is still ongoing [34].

When comparing different ion curves in Fig. 1, we notice three important scalings:

1. At fixed Z, the thermal peaks are shifted to the right linearly in A, i.e, each species thermalizes at a temperature proportional to its mass [19];

2. All the ion spectra rollover at the same E_{max}/Z, consistent with the fact that DSA is a rigidity-dependent process [35];

3. The normalization of the non-thermal spectra at given E/Z is an increasing function of the mass/charge ratio, which implies that the efficiency of injection into DSA depends on A/Z.

The first two results validate the theoretical expectations, while the last one represents the first self-consistent characterization of the parameter that regulates the injection of ions into the DSA process.

Injection enhancement in DSA.— In this section we discuss how the observed boost in ion injection depends on A/Z. The ion non-thermal spectra, neglecting the cutoffs, are power laws that can be written as

$$f_i(E) = \frac{(\gamma - 1) n \chi_i \eta_i}{E_{inj,i}} \left(\frac{E}{E_{inj,i}} \right)^{-\gamma}, \qquad (1)$$

where η_i is the fraction of ions that enter DSA above the injection energy $E_{inj,i}$. We then introduce the ratio

$$K_{ip} \equiv \frac{f_i(E/Z_i)}{\chi_i f_p(E)} = \frac{\eta_i}{\chi_i \eta_p} \left(\frac{E_{inj,i}}{E_{inj,p}} \right)^{\gamma - 1} \qquad (2)$$

as a measure of the enhancement in energetic ions with respect to protons at fixed E/Z. K_{ip} is promptly read from Fig. 1 as the ratio of the normalizations of the power-law spectra. Fig. 2 shows the enhancements obtained for shocks with $\vartheta = 20°$ and $M = \{5, 10, 20, 40\}$; injection fractions and enhancements are calculated by considering the post-shock spectra of species with A/Z up to 8, integrated over $10^3 c/\omega_p$ at time $t = 10^3 \omega_c^{-1}$, when DSA spectra have been established.

For shocks with $M \gtrsim 10$, where accelerated protons generate non-linear upstream magnetic turbulence with $\delta B/B_0 \gtrsim 1$, the fraction of injected particles is $\eta_p \approx 1\%$ for protons and increases linearly with A/Z (top panel); at the same time, $K_{ip} \propto (A/Z)^2$, attesting to a very effective enhancement of particles with large charge/mass (bottom panel). The scaling with A/Z is weaker for the lowest-M shock, for which $\delta B/B_0 \approx 0.2$: η_i is roughly constant at the percent level and $K_{ip} \propto A/Z$.

Chemical enhancements.— The high-M case is relevant for SNR shocks propagating into the warm interstellar medium (ISM), where atoms are typically singly ionized; injected ions will then be stripped of their electrons while undergoing DSA [25]. If GCRs are produced at SNR shocks via DSA [3], our findings may provide an explanation for the chemical enrichment measured in GCRs [5, 7]. In order to compare observations and simulations, we take the observed GCR flux ratios at 1 TeV, $\phi_i(E)$ [e.g., table 1 in ref. 7], weigh them with the fiducial solar abundances, χ_i [8], and write the enhancement at a given E as $K_{ip} Z_i^{1-\gamma}$ (see Eq. 2). We also account for the rigidity-dependent residence time in the Galaxy $\propto (E/Z)^{-\delta}$, with $\delta \simeq 1/3$ above a few GV

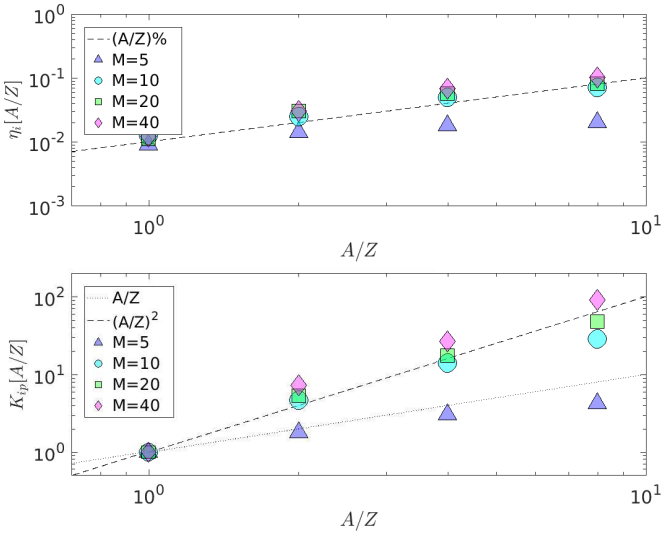

FIG. 2: Preferential acceleration of ions with large A/Z at quasi-parallel shocks with different Mach numbers. For $M \gtrsim 10$ the fraction of injected ions η_i is linear in A/Z (top panel) and the ion enhancement (Eq. 2) scales as $K_{ip} \propto (A/Z)^2$ (bottom panel). For $M = 5$ the self-generated magnetic turbulence is weaker and ion enhancements $K_{ip} \propto A/Z$ only.

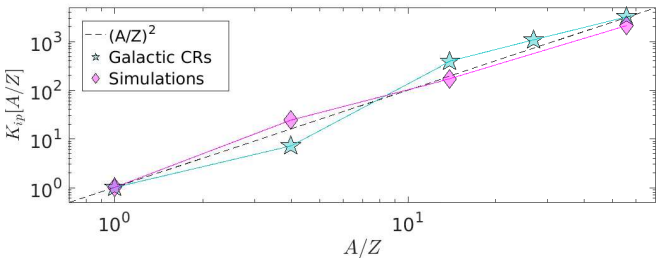

FIG. 3: Chemical enhancements in GCRs (Eq. 3) compared to the ones obtained for a quasi-parallel shock with $M = 20$, assuming that species are singly ionized. The dashed line corresponds to the scaling $\propto (A/Z)^2$ in Fig. 2

[26], and extrapolate the enhancements down to the non-relativistic injection energies. This introduces an additional factor $A_i^{-1/2}$, because DSA spectra are power laws in momentum and hence energy spectra flatten by $E^{1/2}$ at $\sim A_i$GeV. Finally, we obtain that ion injection into DSA must be enhanced at SNR shocks as

$$K_{ip}^{\rm GCRs} = \left.\frac{\phi_i}{\chi_i \phi_p}\right|_{\rm TeV} \frac{Z_i^{\gamma-1-\delta}}{A_i^{1/2}} \simeq \left.\frac{\phi_i}{\chi_i \phi_p}\right|_{\rm TeV} \frac{Z_i^{1/6}}{A_i^{1/2}} \qquad (3)$$

in order to explain the abundances observed in GCRs.

We consider a $M = 20$ and $\vartheta = 20°$ and singly-ionized He, CNO, and Fe atoms with effective $A/Z = \{4, 14, 56\}$ and calculate K_{ip} in the upstream, since at $t = 10^3 \omega_c^{-1}$ ions $A/Z \gtrsim 14$ have already been over-injected but have not yet developed the universal downstream DSA spectrum. The enhancements found in simulations and those in GCR data (Eq. 3) are compared in Fig. 3: the scaling $K_{ip} \simeq (A/Z)^2$ found for strong shocks provides a very good fit, with singly-ionized He, CNO, and Fe particles enhanced by a factor of about ten, hundred, and a few thousand, respectively. The fact that Fe enhancement requires a very large fraction ($\eta_{Fe} \lesssim 50\%$) of the pre-shock particles to enter DSA may have implications for the overall ISM chemical composition, since regions processed by shocks may become depleted in heavy elements. Nevertheless, in the ISM refractory elements are typically trapped in dust grains, so that sputtering may be crucial for their injection [5]. Our results suggest that dust grains with very large $A/Z \gg 1$ should also have no problem in entering DSA, thereby sputtering pre-energized ions [6, 27].

In the low-M regime relevant to heliospheric shocks, our simulations show that DSA may account for enhancements by factors of a few to ten, which are often observed in SEP events [e.g., 10, 28, and references therein]. However, SEP chemical enhancements do not show universal trends in A/Z and/or in the shock inclination and greatly vary from event to event [or even within the same event, see 9]. For instance, the chemical composition of gradual SEPs requires to account for the evolution of the shock inclination as the shock moves outward from the Sun and for the presence of suprathermal seed particles from solar flares [11, 12]. Our simulations, where ion injection into DSA only occurs from the thermal pool, cannot capture the full phenomenology of heliospheric shocks, but still represent a solid benchmark for singling out the additional role of pre-energized seed particles in these environments [36].

Oblique Shocks.— **Shocks with $\vartheta \gtrsim 50°$ cannot inject *thermal* protons and spontaneously drive self-generated magnetic turbulence [21, 24], but can act as accelerators if energetic particle seeds are already present in the upstream. We ran simulations of oblique shocks ($\vartheta = 60°$) and found that ions with large A/Z thermalize at a temperature $\propto A$, but progressively further in the downstream with respect to the quasi-parallel case. Neither protons nor heavier ions develop non-thermal tails, which means that having a large gyroradius ($\propto A/Z$) is not a *sufficient* condition for being injected into DSA. Moreover, this confirms that, regardless of the local inclination where CRs are accelerated, the relative CR abundances are fully determined by the physics of ion injection in quasi-parallel shock regions only.**

The injection mechanism.— Proton injection is due to specular reflection off the time-dependent potential barrier at the shock and energization via shock-drift acceleration (SDA) [24]. Unlike protons, heavy ions are not

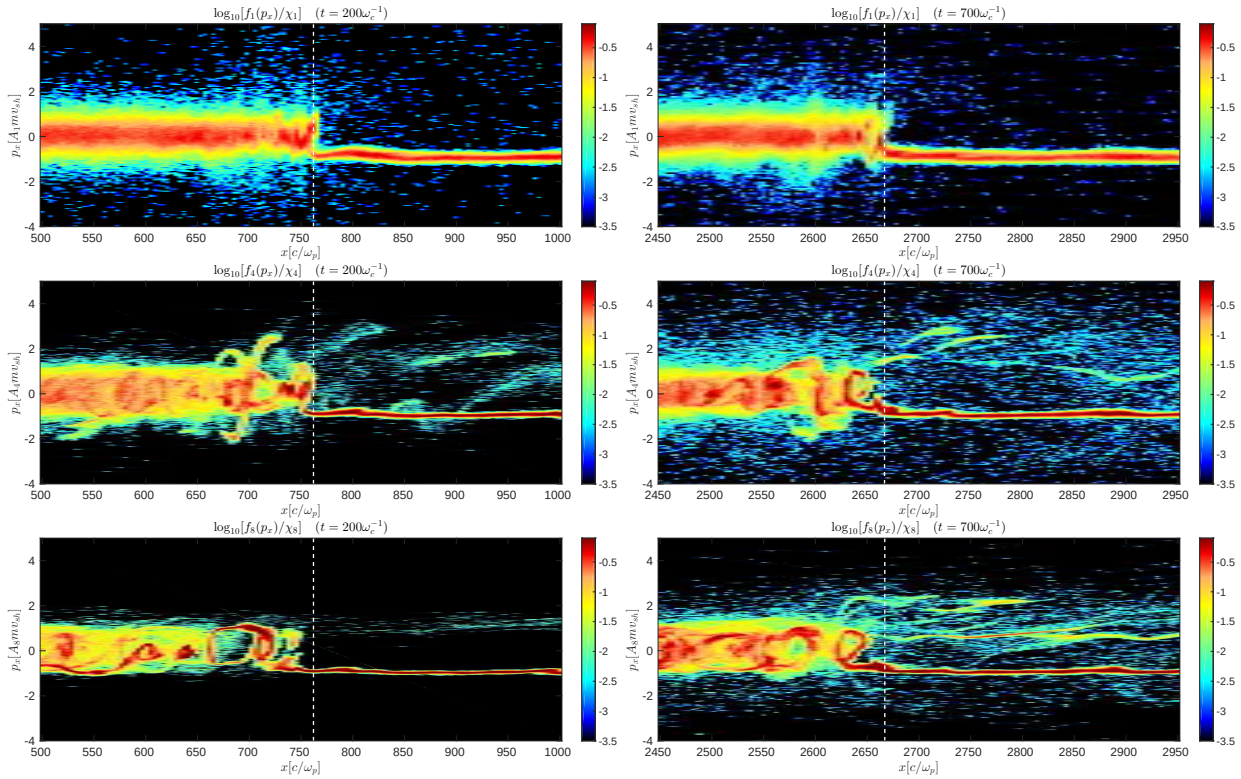

FIG. 4: $x - p_x$ phase space at $t = \{200, 700\}\omega_c^{-1}$ (left to right) for our benchmark case; top to bottom panels correspond to species with $A/Z = \{1, 4, 8\}$, respectively. Ions with larger A/Z isotropize further downstream of the shock marked with dashed lines. At $t = 200\omega_c^{-1}$ energetic protons are already diffusing, ions with $A/Z = 4$ have just started being injected, and ions with $A/Z = 8$ are still anisotropic and not injected. At $t = 700\omega_c^{-1}$, instead, all species exhibit typical DSA spectra.

halted by the shock barrier and penetrate downstream, where their distribution tends to become more isotropic due to rapidly-varying fields. If isotropization is rapid enough with respect to advection, there arises a population of backstreaming ions that can overrun the shock barrier. The fraction of injected heavy ions is thus controlled by how rapid the isotropization is, which depends on A/Z and on the self-generated magnetic turbulence, as demonstrated by the scaling of chemical enhancements with M and ϑ [22].

Fig. 4 shows the $x-p_x$ phase spaces for our benchmark run; we consider ions with $Z = 1$ and $A = \{1, 4, 8\}$ at times $t = \{200, 700\}\omega_c^{-1}$. We see that, while protons are promptly isotropized at the shock, ions with larger A retain their anisotropy further in the downstream. At early times (left column), protons show the characteristic non-thermal, isotropic population of diffusing particles [21]. Ions with $A/Z = 4$ have just started overrunning the shock, but there are only few particles with $p_x < 0$ in the upstream, implying that DSA has not yet been established. Finally, ions with $A/Z = 8$ isotropize far downstream and are not injected. At later times ($t = 700\omega_c^{-1}$, right column) all of the species show the typical DSA spectrum comprising non-thermal diffusing particles.

Proton injection is controlled by the quasi-periodic reformation of the shock barrier [24]; **instead, injection of heavier ions happens at later times for heavier species (always after the onset of nonlinear turbulence) and relies on small-scale, non-adiabatic, rapid electromagnetic fluctuations with amplitude larger than those induced by the local shock reformation.** Such a scenario is *not* equivalent to the *thermal leakage* model for particle injection [e.g., 29–31], in that the injected ions are not the most energetic in the tail of the Maxwellian (strictly speaking, they have not yet thermalized).

In summary, while injected protons are reflected by the shock barrier and need to be pre-energized via few cycles of SDA [24], heavy ions reflect off post-shock self-generated magnetic irregularities. The enhancement in ions with $A/Z \gg 1$ is then due to the fact that they are not affected by the proton-regulated shock barrier; they do not experience SDA but rather start diffusing right away. Ions with $A/Z \gtrsim 1$ exhibit intermediate properties because their probability of being reflected or transmitted at the shock barrier depends on the actual angle between their momentum and the shock normal [24].

Conclusions.— We have presented the first ab-initio

calculation of ion DSA at non-relativistic shocks, finding that species with large A/Z show enhanced non-thermal tails with respect to protons, in quantitative agreement with the chemical abundances observed in GCRs. In forthcoming publications we will discuss the implications of these findings also for the *discrepant hardening* of non-H species in GCRs [e.g., 32] and for the role of accelerated He in SNR shocks [7].

This research was supported by NASA (grant NNX17AG30G to DC), NSF (grant AST-1714658 to DC and grant AST-1517638 to AS), and Simons Foundation (grant 267233 to AS). Simulations were performed on computational resources provided by the Princeton High-Performance Computing Center, the University of Chicago Research Computing Center, and XSEDE TACC (TG-AST100035).

[1] D. Caprioli, E. Amato, and P. Blasi, APh **33**, 160 (2010), 0912.2964.
[2] G. Morlino and D. Caprioli, A&A **538**, A81 (2012), arXiv:1105.6342.
[3] D. Caprioli, ArXiv:1510.07042 (2015), 1510.07042.
[4] J. A. Simpson, Annual Review of Nuclear and Particle Science **33**, 323 (1983).
[5] J. Meyer, L. O. Drury, and D. C. Ellison, ApJ **487**, 182 (1997), astro-ph/9704267.
[6] D. C. Ellison, L. O. Drury, and J.-P. Meyer, Astrophys. J. **487**, 197 (1997), astro-ph/9704293.
[7] D. Caprioli, P. Blasi, and E. Amato, APh **34**, 447 (2011), 1007.1925.
[8] K. Lodders, Astrophys. J. **591**, 1220 (2003).
[9] D. V. Reames, SSRev **194**, 303 (2015), 1510.03449.
[10] M. I. Desai, G. M. Mason, M. A. Dayeh, R. W. Ebert, D. J. Mccomas, G. Li, C. M. S. Cohen, R. A. Mewaldt, N. A. Schwadron, and C. W. Smith, Astrophys. J. **816**, 68 (2016).
[11] A. J. Tylka, C. M. S. Cohen, W. F. Dietrich, M. A. Lee, C. G. Maclennan, R. A. Mewaldt, C. K. Ng, and D. V. Reames, Astrophys. J. **625**, 474 (2005).
[12] A. J. Tylka and M. A. Lee, Astrophys. J. **646**, 1319 (2006).
[13] A. R. Bell, MNRAS **182**, 147 (1978).
[14] R. D. Blandford and J. P. Ostriker, ApJL **221**, L29 (1978).
[15] D. C. Ellison, E. Moebius, and G. Paschmann, Ap. J. **352**, 376 (1990), URL `http://adsabs.harvard.edu/abs/1990ApJ...352..376E`.
[16] D. Eichler and K. Hainebach, Physical Review Letters **47**, 1560 (1981).
[17] D. Burgess, GRL **16**, 163 (1989).
[18] K. J. Trattner and M. Scholer, GRL **18**, 1817 (1991).
[19] Y. A. Kropotina, A. M. Bykov, A. M. Krasil'shchikov, and K. P. Levenfish, Journal of Technical Physics **61**, 517 (2016).
[20] L. Gargaté, R. Bingham, R. A. Fonseca, and L. O. Silva, Comp. Phys. Commun. **176**, 419 (2007), arXiv:physics/0611174.
[21] D. Caprioli and A. Spitkovsky, Astrophys. J. **783**, 91 (2014), 1310.2943.
[22] D. Caprioli and A. Spitkovsky, Astrophys. J. **794**, 46 (2014), 1401.7679.
[23] D. Caprioli and A. Spitkovsky, Astrophys. J. **794**, 47 (2014), 1407.2261.
[24] D. Caprioli, A. Pop, and A. Spitkovsky, ApJL **798**, 28 (2015), 1409.8291.
[25] G. Morlino, Physical Review Letters **103**, 121102 (2009), 0908.3217.
[26] P. Blasi and E. Amato, JCAP **1**, 10 (2012), 1105.4521.
[27] J. D. Slavin, E. Dwek, and A. P. Jones, Astrophys. J. **803**, 7 (2015), 1502.00929.
[28] G. M. Mason, J. E. Mazur, and J. R. Dwyer, ApJL **525**, L133 (1999).
[29] J. P. Edmiston, C. F. Kennel, and D. Eichler, GRL **9**, 531 (1982).
[30] M. A. Malkov, Phys. Rev. E **58**, 4911 (1998), arXiv:astro-ph/9806340.
[31] P. Blasi, S. Gabici, and G. Vannoni, MNRAS **361**, 907 (2005), astro-ph/0505351.
[32] H. S. Ahn et al. [CREAM Collaboration], ApJL **714**, L89 (2010), URL `http://stacks.iop.org/2041-8205/714/i=1/a=L89`.
[33] D. C. Ellison and R. Ramaty, Astrophys. J. **298**, 400 (1985).
[34] We checked that chemical enhancements do not depend on the electron equation of state and that $\mathcal{E}_i \propto A_i$ for all species, including protons, if the electron pressure is set to zero.
[35] While rigidity is defined as p/Z, the acceleration time does scale as E/Z in the non-relativistic case [23, 33].
[36] Note that seeds can be injected into DSA also at oblique shocks.